Vol 18 No 11, November 2009
1674-1056/2009/18(11)/4807-08

Chinese Physics B

© 2009 Chin. Phys. Soc.
and IOP Publishing Ltd

# Ionization of atoms by chirped attosecond pulses*

Tan Fang(谭 放), Peng Liang-You(彭良友)†, and Gong Qi-Huang(龚旗煌)‡

*State Key Laboratory for Mesoscopic Physics and Department of Physics, Peking University, Beijing* 100871, *China*

(Received 19 December 2008; revised manuscript received 23 March 2009)

We investigate the ionization dynamics of atoms by chirped attosecond pulses using the strong field approximation method. The pulse parameters are carefully chosen in the regime where the strong field approximation method is valid. We analyse the effects of the chirp of attosecond pulses on the energy distributions and the corresponding left-right asymmetry of the ionized electrons. For a single chirped attosecond pulse, the ionized electrons can be redistributed and the left-right asymmetry shows oscillations because of the introduction of the chirp. For time-delayed double attosecond pulses at different intensities with the weaker one chirped, exchanging the order of the two pulses shows a relative shift of the energy spectra, which can be explained by the different effective time delays of different frequency components because of the chirp.

**Keywords:** photoionization rate, attosecond pulse, asymmetry, chirp
**PACC:** 3280, 3280F, 3380K, 4265

## 1. Introduction

With the fast development of femtosecond laser technologies, phase-stabilized few-cycle and even single-cycle laser pulses can be routinely obtained in many laboratories.[1] Using these intense femtosecond laser pulses, a single attosecond pulse or a train of attosecond pulses can be generated in many research groups through high-order harmonic generation (HHG) occurring in highly nonlinear interactions with matter.[2,3] The shortest attosecond pulse of 80 as at a photon energy around 80 eV was recently obtained by Goulielmakis *et al.*[4]

Chirp pulse amplification (CPA) technology has been widely used to generate ultra-intense and ultrashort laser pulses.[5] For chirped femotosecond pulses in the infrared region, many novel phenomena have been found in the dynamics of excitation, ionization, and dissociation of atoms and molecules.[6−8] In the attosecond pulse generation process, chirp is inherent,[9] although the chirp is usually partially compensated by metal foils in order to achieve shorter pulses. In the present work, we study the effects of the chirp of an attosecond pulse on the ionization dynamics of atoms. Chirped attosecond pulses have been used in a pump-probe scheme of atomic dynamics which has been studied by Yulin and coworkers.[10] However, the purpose of this study is to investigate how the chirp will change the ionization dynamics and how one can use the chirp as an additional tool to control the electronic dynamics of the atoms and molecules in the interaction with attosecond pulses.

The strong field approximation (SFA) has been widely used to explain many strong field phenomena, including the above-threshold ionization (ATI).[11−15] To explain the plateau observed in ATI,[16,17] the high order term in the $S$-matrix has to be considered, which corresponds to the rescattering process of the ionized electrons with the ionic core.[18−20] In appropriate laser parameters and with careful treatment of the transition matrix, SFA is still successfully used by many authors to explain a lot of novel phenomena in strong field physics.[21−24]

In the present work, we are interested in the atomic ionization dynamics by a chirped attosecond pulse whose central frequency is well above the ionization threshold and the full width at half maximum (FWHM) of the pulse is as short as a few optical cycles. Therefore, the ionized electrons have a large initial velocity and we are interested only in the direct one-photon process where the rescattering with the ionic core can be ignored. Judging by the Keldysh parameter, the electrons are mainly ionized in the multi-photon regime. Therefore, it is a little misleading to use the terminology 'strong field approximation'. However, as we will show below, the

*Project supported by the National Natural Science Foundation of China (Grant Nos 10704003 and 10821062) and the National Basic Research Program of China (Grant No 2006CB806007).
†E-mail: liangyou.peng@pku.edu.cn
‡E-mail: qhgong@pku.edu.cn

calculated transition matrix from the atomic ground state to the continuum state looks very similar to the form of the first-order SFA. Indeed, there are already quite a few publications applying similar SFA methods for the ionization dynamics by attosecond pulses or by attosecond pulses with an additional infrared pulse.[25−28] We thus believe that the application of SFA to chirped attosecond pulses in the present study is able to capture much of the important physical essence.

The rest of our paper is organized as follows. We first give a brief introduction to the SFA method and introduce our chirped Gaussian laser pulse. Then we will present the energy distributions and the corresponding left-right asymmetry of the ionized electrons. Finally, we will conclude our main results and present a short discussion.

## 2. Numerical method

In this paper, we consider a chirped Gaussian pulse, which has been used by many other authors.[6−8,10] The laser pulse is assumed to be linearly polarized along the $z$ axis and its vector potential is given by

$$\boldsymbol{A}(t) = A_0 F(t) \cos\left[\omega_0(t-t_0) + 4\ln 2\frac{(t-t_0)^2}{\tau_0^2}\frac{\xi}{1+\xi^2} + \phi_0\right]\boldsymbol{e}_z, \tag{1}$$

with the envelop

$$F(t) = \exp\left[-4\ln 2\frac{(t-t_0)^2}{\tau_0^2}\frac{1}{1+\xi^2}\right] = \exp\left[-4\ln 2\frac{(t-t_0)^2}{\tau^2}\right]. \tag{2}$$

In the above equations, the parameter $\xi$ stands for the dimensionless linear chirp rate. When $\xi = 0$, the pulse is a Fourier transform limited pulse with FWHM $\tau_0$. The FWHM $\tau$ of the chirped pulse is given by the equation

$$\tau = \tau_0\sqrt{1+\xi^2}. \tag{3}$$

The electric field strength $\boldsymbol{E}(t)$ of the laser pulse is then calculated by the time derivative of the vector potential

$$\boldsymbol{E}(t) = -\frac{\partial \boldsymbol{A}(t)}{\partial t}. \tag{4}$$

Note that, in the present study, we take the peak values of the vector potential as follows:

$$A_0 = \frac{E_0}{\omega_0} = \frac{1}{\omega_0}\sqrt{\frac{I_0/I_{\rm au}}{\sqrt{1+\xi^2}}}, \tag{5}$$

where $I_0$ is the peak intensity of the unchirped pulse and $I_{\rm au} = 3.51\times10^{16}$ W/cm$^2$ is the atomic unit of the laser intensity. We use Eq.(5) in order to simulate the realistic experimental case where the introduction of the chirp $\xi$ means that the duration of the pulse increases to $\tau_0\sqrt{1+\xi^2}$ and the intensity of the pulse decreases to $I_0/\sqrt{1+\xi^2}$, but with the total pulse energy fixed.

According to the SFA method,[29] the transition amplitude of an atomic electron from the initial state $\psi_{\rm i}(\boldsymbol{r})$ at time $t_0$ to a continuum state $\psi_{\boldsymbol{p}}(\boldsymbol{r})$ at time $t$ with momentum $\boldsymbol{p}$ can be expressed in the $S$-matrix formulism as

$$M_{p\rm i} = -\,{\rm i}\lim_{t\to\infty}\int_{-\infty}^{t}{\rm d}t_0 < \psi_{\boldsymbol{p}}(t)|U(t,t_0) \times \boldsymbol{r}\cdot\boldsymbol{E}(t_0)|\psi_{\rm i}(t_0)\rangle, \tag{6}$$

where $U(t,t_0)$ is the time evolution operator of the complete Hamiltonian

$$\begin{aligned} H(t) &= H_{\rm a} + H_{\rm i}(t) \\ &= -\frac{1}{2}\nabla^2 + V(r) + H_{\rm i}(t) \\ &= -\frac{1}{2}\nabla^2 + V(r) + \boldsymbol{r}\cdot\boldsymbol{E}(t), \end{aligned} \tag{7}$$

with $H_{\rm a}$ being the field-free atomic Hamiltonian, $H_{\rm i}(t)$ being the laser–atom interaction Hamiltonian in the dipole approximation and length gauge description and $V(r)$ being the short range Yukawa potential given in Ref.[29]. It is well known that $U(t,t_0)$ satisfies the Dyson equation

$$U(t,t_0) = U_L(t,t_0) - {\rm i}\int_{t_0}^{t}{\rm d}t' U_{\rm L}(t,t')V(r)U(t',t_0). \tag{8}$$

Substituting Eq.(8) into Eq.(6), one can write the transition amplitude $M_{p\rm i}$ into two parts

$$M_{p\rm i} = M_{p\rm i}^{(0)} + M_{p\rm i}^{(1)}, \tag{9}$$

where $M^{(0)}$ is the direct ionization probability amplitude and $M_{pi}^{(1)}$ denotes the rescattering ionization probability amplitude. In Eq.(8), $U_{\rm L}(t,t_0)$ is the time evolution operator for the Hamiltonian of a free electron in the laser field

$$H_{\rm L} = -\frac{1}{2}\nabla^2 + \boldsymbol{r}\cdot\boldsymbol{E}. \tag{10}$$

In the present study, the photon energy is chosen to be much higher than the ionization threshold and the FWHM of the laser pulse is as short as a few optical cycles. Therefore, the atomic excitation states do not play significant roles and we are only interested in the direct ionization process where the rescattering of the ionized electron with the core is negligible. For these reasons, we simply drop the rescattering term $M_{pi}^{(1)}$ and just consider the direct ionization amplitude

$$M_{pi}^{(0)} = -\,{\rm i}\lim_{t\to\infty}\int_{-\infty}^{t}{\rm d}t_0 < \psi_{\boldsymbol{p}}^{(L)}(t)|U_{\rm L}(t,t_0) \times \boldsymbol{r}\cdot\boldsymbol{E}(t_0)|\psi_{\rm i}(t_0)\rangle, \tag{11}$$

where the final state $|\psi_{\boldsymbol{p}}^{(\rm L)}(t)\rangle$ is the Volkov state (the eigenstate of $H_{\rm L}$)

$$|\psi_{\boldsymbol{p}}^{(\rm L)}(t)\rangle = |\boldsymbol{p}+\boldsymbol{A}(t)\rangle\exp\left[-\,{\rm i}\,S_{\boldsymbol{p}}(t)\right], \tag{12}$$

with the phase

$$S_{\boldsymbol{p}}(t) = \frac{1}{2}\int^{t}{\rm d}t'[\boldsymbol{p}+\boldsymbol{A}(t')]^2. \tag{13}$$

For the laser parameters we are interested in, the ionized electrons have a large net momentum. It is known that, for larger wave numbers, it is better in approximating a Coulomb wave as a plane wave. So the effect of the Coulomb potential in the continuum states is neglected, which is standard in the SFA type of method.[20]

The initial state $|\psi_{\rm i}(t_0)\rangle$ is taken to be the ground state of a hydrogenic atom

$$\psi_{\rm i}(t_0) = 2Z^{3/2}\exp\left(-Zr\right)Y_{00}(\hat{r}){\rm e}^{{\rm i}\,I_{\rm p}t_0}, \tag{14}$$

where $I_{\rm p}$ is the atomic ionization potential.

Substituting Eqs.(14) and (12) into Eq.(11), we can obtain the direct ionization probability amplitude $M_{pi}^{(0)}$ as the following[29]

$$M_{pi}^{(0)}(\boldsymbol{p}) = -\frac{8\sqrt{2}Z^{5/2}}{\pi}\int_{-\infty}^{\infty}{\rm d}t\frac{\boldsymbol{E}(t)\cdot[\boldsymbol{p}+\boldsymbol{A}(t)]}{\{[\boldsymbol{p}+\boldsymbol{A}(t)]^2+Z^2\}^3} \times {\rm e}^{{\rm i}[S_{\boldsymbol{p}}(t)+I_{\rm p}t]}. \tag{15}$$

We note that the above formula for the transition matrix is very similar to those used in Refs.[25]–[27]. In these references, these kinds of SFA methods gave a very nice description of what they observed in the experiments. However, in their cases, the phase factor $S_{\boldsymbol{p}}(t)$ is calculated by the IR pulse since the contribution of the attosecond pulse is very small compared to that of the IR pulse. For the present case where one only has attosecond pulses, $S_{\boldsymbol{p}}(t)$ is calculated by attosecond pulses. It is well known that in the XUV+IR streaking type of experiments, the atoms are mainly ionized by the attosecond pulses and the IR pulse only shifts the electronic wave packets in the momentum space as a whole by a value of the IR vector potential at the time of birth of the ionizing electronic wave packets.

When the laser is linearly polarized, the momentum distributions are axisymmetric with the $z$-axis. So we only consider that the ionized electron is in a plane in momentum space, thus one can assume $k_y = 0$.[30] The direct ionization probability can then be obtained as the following equation

$$P(E,\theta_k) = |M_{pi}^{(0)}(\boldsymbol{p})|^2, \tag{16}$$

where $E$ is the final electron energy and $\theta_k$ is the angle between the electron ejection and the laser polarization direction $e_z$. We define the unnormalized left-right asymmetry as

$$P(E) = P(E,\pi) - P(E,0), \tag{17}$$

which is the difference of ionization probabilities antiparallel ($\theta_k = \pi$) and parallel ($\theta_k = 0$) to the laser polarization.

## 3. Results and analysis

In this section, we will present the energy distributions and the left-right asymmetry of the electrons ionized by chirped attosecond pulses. We have set $Z = 1$ in Eq.(14) and the ionization potential $I_{\rm p} = 0.5$ a.u., corresponding to those of the hydrogen atom. In the following calculations, we have chosen the central frequency of the chirped attosecond pulse $\omega_0 = 1.0$ a.u., the carrier envelope phase (CEP) of the pulse $\phi_0 = 0.5\pi$, and the FWHM of the unchirped pulse $\tau_0 = 1.2T_0$, where we define $T_0$ as the optical period of the unchirped pulse $T_0 = 2\pi/\omega_0$. The laser pulse intensities are shown in terms of the unchirped pulse, either $I_0 = 5\times10^{13}$ W/cm$^2$ or $3\times10^{15}$ W/cm$^2$, the peak intensity of the chirped pulse is reduced according to $I_0/\sqrt{1+\xi^2}$. We focus only on the direct one-photon peak around an electron energy around

0.5 a.u. where the rescattering of the electrons with the core does not play any significant role.

In Fig.1, we present the energy distributions of the electrons ionized by an attosecond pulse along the laser polarization at a low intensity of $I_0 = 5 \times 10^{13}$ W/cm$^2$ and a higher intensity of $I_0 = 3 \times 10^{15}$ W/cm$^2$ for different values of the chirp rate $\xi$. For the first row where $\xi = 0$, we obtain very similar results to those calculated by a direct solution of the time dependent Schrödinger equation (TDSE),[30,31] i.e., one observes left-right asymmetry of the energy spectra only at sufficiently high laser intensities. So it validates again that the SFA method is suitable to be used here. For the higher intensity of $I_0 = 3 \times 10^{15}$ W/cm$^2$ at the right column, it appears that the left-right asymmetry becomes much smaller as the $\xi$ becomes nonzero in Fig.1, compared with Fig.1(d). Actually, this is because the actual peak intensity of the chirped laser pulse is decreased to $1.5 \times 10^{15}$ W/cm$^2$. Compared with Fig.1(d) where the two curves intersect once around 0.4 a.u., the two curves in Fig.1(e) intersect almost 5 times because of the introduction of the chirp to the laser pulse. Actually, as one increases the chirp from 1.732 to 2.828 in Fig.1(f), there turn out to be many more intersections between the two curves, although the actual laser peak intensity is further reduced to $1.0 \times 10^{15}$ W/cm$^2$. We point out that, for the left column at the much lower intensity of $5 \times 10^{13}$ W/cm$^2$, there actually appear also very interesting intersections as for the higher intensity case, but they are not easily identified in the scale of this figure.

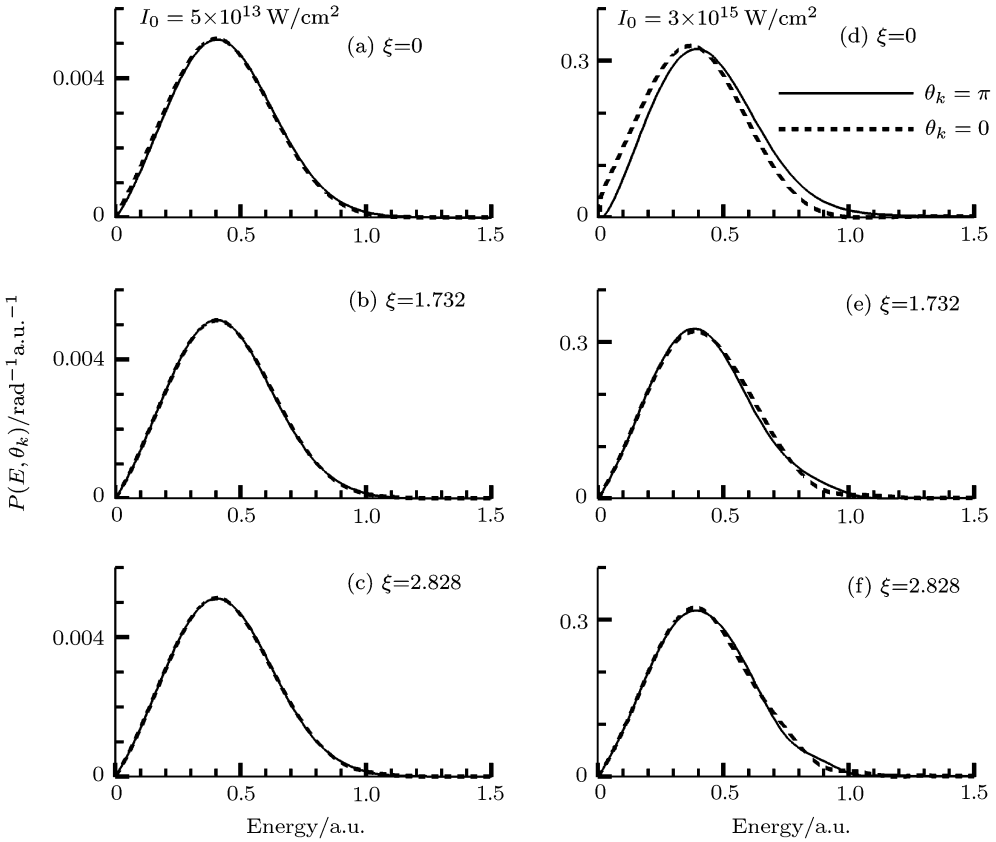



**Fig.1.** The electron energy spectra at the angle $\theta_k = 0$ (dotted lines) and $\theta_k = \pi$ (solid lines) at the peak intensity $I_0 = 5 \times 10^{13}$ W/cm$^2$ (left column) and $I_0 = 3 \times 10^{15}$ W/cm$^2$ (right column) with various chirp rates $\xi$. The FWHM of the pulse is $\tau_0\sqrt{1+\xi^2}$ with $\tau_0 = 1.2T_0$. As can be clearly seen in (f), the chirp of the attosecond pulse introduces oscillations in the energy spectra: the two curves intersect several times.

For the purposes of clearer presentation of these new phenomena introduced by the chirped attosecond pulse, we show in Fig.2 the unnormalized left-right asymmetry $P(E)$ defined in Eq.(17). In this figure, the points where $P(E)$ changes its sign correspond to the intersections of the left and right electron energy spectra shown in Fig.1. As we can see from the comparison of the left and right column in Fig.2, the shapes of the $P(E)$ are very similar for the same chirp rate $\xi$, although their values differ by several orders of magnitude because of the big difference in laser peak intensities. There is only one intersection around 0.4 a.u. when $\xi = 0$. As one increases $\xi$ to 1.732 and 2.828, the number of the intersections increases to 5 and 8 respectively. We have to emphasize that the increase of the intersections is not just due to the increase of the pulse length after one introduces the chirp. We have done calculations with the same peak intensities and pulse durations as those in Figs.2(b), 2(c), 2(e) and 2(f), but with the chirp rate $\xi = 0$. The results indeed also show a slight increase of the intersections, but not as many as those shown in Fig.2 when the chirp rate is not zero. Also, the distributions of the intersections are not regularly distributed as those in Fig.2 are. This evidence tells us that the chirp of the attosecond pulses rearranges the different frequency components contained in the short pulses and brings new features in the energy spectra of the ionized electrons. In other words, the introduction of the chirp can redistribute the ionized electrons in a certain regular way.

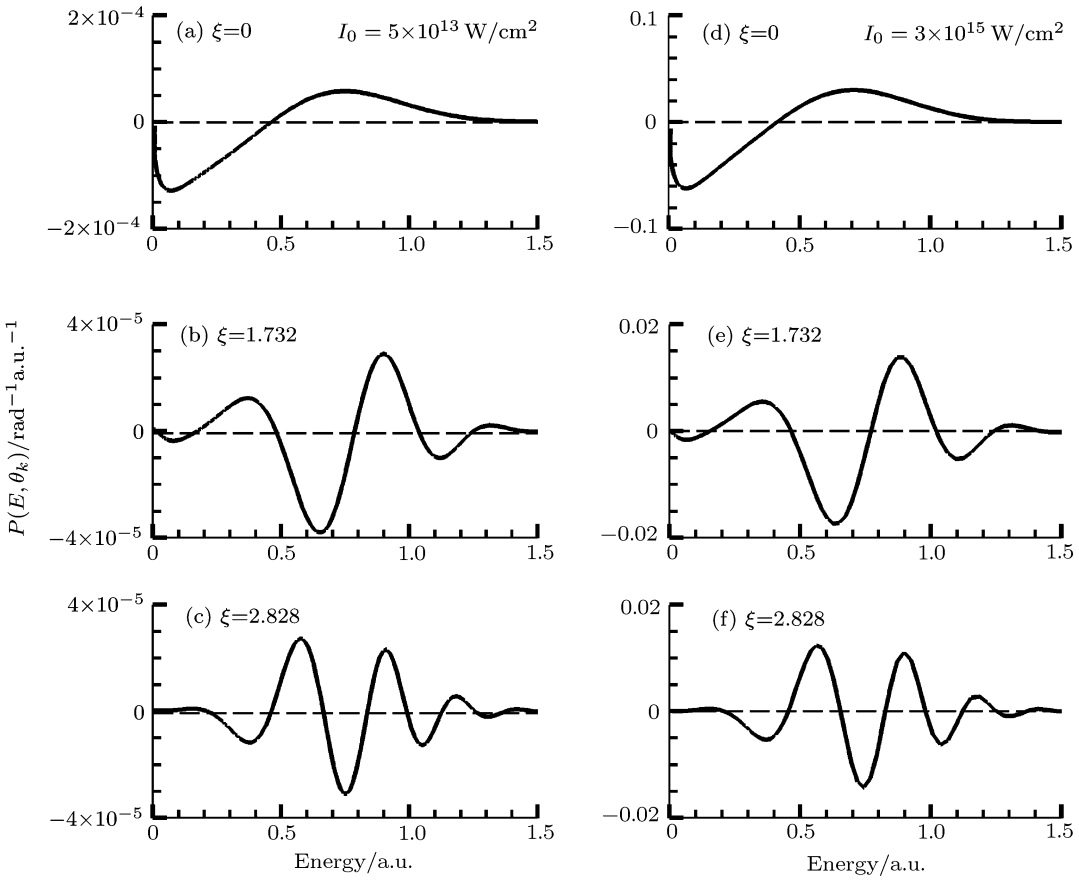



**Fig.2.** The left-right asymmetry $P(E) = P(E,\pi) - P(E,0)$ with the same laser parameters as Fig.1. One notices that the chirp of the attosecond pulse introduces very interesting oscillations of the left-right asymmetry: the larger the $\xi$, the faster the oscillation. The dashed lines are drawn to guide one's eye for the number of intersections with $P(E) = 0$.

Now let us turn to consider the case where the atom is ionized by relatively-delayed double attosecond pulses. In Fig.3, we present the energy spectra in the direction $\theta_k = \pi$ for double pulses with an intensity $I_0$ equal to $5 \times 10^{13}$ W/cm$^2$ and $3 \times 10^{15}$ W/cm$^2$, respectively. In the results presented in Fig.3, we only let the weaker pulse ($5 \times 10^{13}$) chirped with the value of $\xi$ indicated in each panel, but the stronger pulse ($3 \times 10^{15}$) is always not chirped ($\xi = 0$). In order to show the effects of the introduction of chirp for the weaker pulse, we have chosen the same time delay $T_{\rm d} = 18.16T_0$ between the centres of the envelopes of the two pulses. The solid curves in each panel of Fig.3 show the energy spectra when the weaker pulse is applied before the stronger pulse, while the dashed curves show the energy spectra when the weaker pulse is applied after the stronger pulse. As one can see from Fig.3(a), when both pulses are not chirped, exchanging the order of the two pulses does not change the ionized electron spectra at all. The oscillation patterns in the energy spectra result in interference between the two ionizing electronic wave packets produced by the time delayed double pulses, as has also been observed by the direct solution of the TDSE.[30]

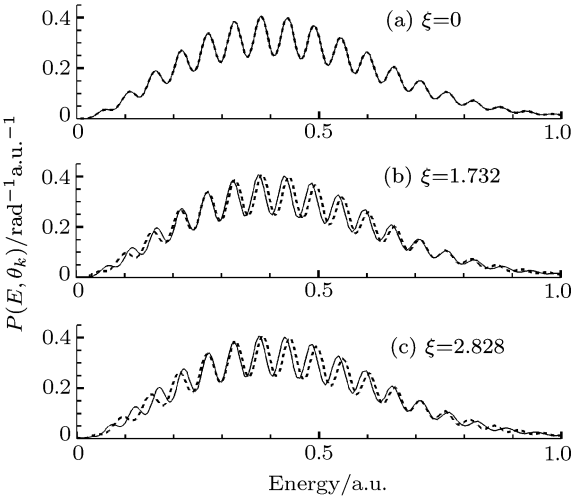



**Fig.3.** The energy spectra of electrons ionized by two laser pulses with intensities of $5 \times 10^{13}$ W/cm$^2$ and of $3 \times 10^{15}$ W/cm$^2$, with the weaker one chirped at different rates $\xi$, indicated. We only consider the spectra at the direction $\theta_k = \pi$. The solid curves show results when the chirped weaker pulse is applied before the unchirped stronger one, and the dotted curves show those results when the chirped weaker pulse is applied after the unchirped stronger one. In all cases shown above, the two pulses have a FWHM of $\tau_0\sqrt{1+\xi^2}$ with $\tau_0 = 1.2T_0$ and the same time delay of $T_{\rm d} = 18.16T_0$.

The period of the oscillations is $2\pi/T_{\rm d}$, as explained in Ref.[30]. For the present case where $T_{\rm d} = 18.16T_0$, the oscillation is about 0.055 a.u., which is consistent with the prediction of this simple formula.

However, the interesting point in Fig.3 is that, when one exchanges the order of the two laser pulses, the energy spectra do not overlap any more as in Fig.3(a) if the weaker pulse is chirped. As can be seen from Figs.3(b) and 3(c), the small peaks around energy 0.27 a.u. stay almost the same, but the dotted curves shift leftwards and rightwards respectively for smaller and larger electron energy, with respect to the solid curve when the weaker pulse is applied ahead of the stronger pulse. This is because the chirp of the pulse will redistribute the frequency components, i.e., the lower frequencies come first and the higher frequencies come at later times if the pulse has a positive chirp rate.

Figure 4 shows the effects of the chirp rate on the shift of the spectra. For the present case, the weaker pulse has a positive chirp, which results in the fact that the different frequency components interact with the atom at different times. Considering a frequency component $\omega_0 + \Delta\omega$, we define the time delay $T_{\rm d}(\Delta\omega)$ between these components in the unchirped pulse and chirped pulse. Then, $T_{\rm d}(\Delta\omega)$ changes with $\Delta\omega$. According to Eq.(1), one can obtain the time centre of the frequency component $\omega_0 + \Delta\omega$ in the chirped pulse as

$$t_1 = t_0 + \frac{\Delta\omega\tau^2}{4\ln 2}\frac{1+\xi^2}{\xi}, \tag{18}$$

and its time centre in the unchirped pulse as

$$t_2 = t_0 + 18.16T_0. \tag{19}$$

So the time delay $T_{\rm d}(\Delta\omega)$ is

$$T_{\rm d}(\Delta\omega) = t_2 - t_1 = 18.16T_0 - \frac{\Delta\omega\tau^2}{4\ln 2}\frac{1+\xi^2}{\xi}. \tag{20}$$

When $\xi > 1.0$, the time delay $T_{\rm d}$ decreases with the increase of chirp rate $\xi$. So the delay for $\xi = 1.732$ is bigger than the delay for $\xi = 2.828$ but both of them are smaller than that for $\xi = 0$, which is $18.16T_0$.

Exchanging the order of the two pulses, i.e., the chirped weaker pulse is applied after the stronger one, the effective time delay for the frequency component $\omega_0 + \Delta\omega$ is

$$T_{\rm d}(\Delta\omega) = 18.16T_0 + \frac{\Delta\omega\tau^2}{4\ln 2}\frac{1+\xi^2}{\xi}. \qquad (21)$$

When $\xi > 1.0$, the time delay $T_{\rm d}$ increases with the increase of chirp rate $\xi$. So the delay for $\xi = 1.732$ is smaller than the delay for $\xi = 2.828$ but both of them are larger than that for $\xi = 0$.

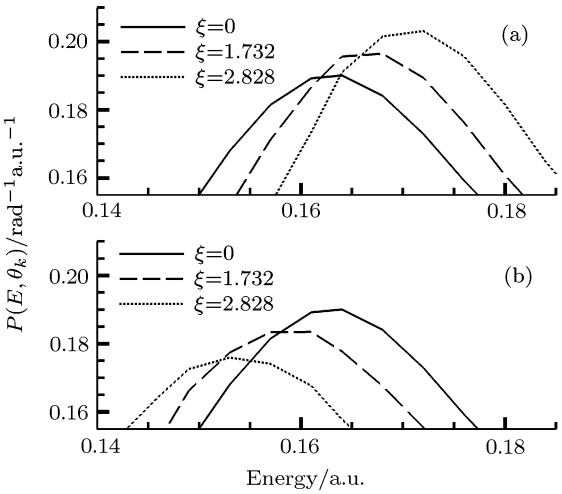



**Fig.4.** Enlarged portions of the energy spectra in the direction $\theta_k = \pi$ from 0.14 a.u. to 0.19 a.u. for different values of chirp $\xi$ of the weaker pulse: (a) the chirped weaker pulse is applied first; (b) the unchirped stronger pulse is applied first. As in Fig.3, we only consider the the spectra in the direction $\theta_k = \pi$.

The different effective time delays $T_{\rm d}$ lead to different interference patterns in the energy spectrum when one exchanges the order of the two pulses. These are clearly seen in Fig.4 where the energy spectra from 0.14 a.u. to 0.19 a.u. are shown for different chirp rates $\xi$.

# 4. Conclusion and outlook

In summary, we have studied the energy spectra and their left-right asymmetry produced by chirped attosecond pulses. When the atom is ionized by a single chirped attosecond pulse, the oscillation of the left-right asymmetry will become faster with the increase of chirp rate, reflecting the redistribution of the ionized electrons. When the atom is ionized by two laser pulses with one of them chirped, exchanging the order of them will produce different energy spectra, which can be explained by the different effective time delays between the frequency components in the chirped pulse and the unchirped one.

We have only considered the cases where the central frequency is well above the atomic ionization potential and also focused only on the direct one-photon peak where the strong field approximation method works. One expects that, when the photon energy is near the ionization threshold, which is 0.5 a.u. for hydrogen, the electrons will have a probability of being excited to higher excited states by the low frequency components of the attosecond pulse and thus a double pulse study will lead to much more interesting physics. But this is beyond the SFA method where the excited states are completely neglected and the Coulomb potential is ignored; we are carrying out more detailed studies using the direct solution of the TDSE.

# References


[1] Brabec T and Krausz F 2000 *Rev. Mod. Phys.* **72** 545

[2] Paul P M, Toma E S, Breger P, Mullot G, Augé F, Balcou P, Muller H G and Agostini P 2001 *Science* **292** 1689

[3] Christov I P, Murnane M M and Kapteyn H C 2000 *Opt. Expess* **7** 362

[4] Goulielmakis E, Schultze M, Hofstetter M, Yakovlev V S, Gagnon J, Uiberacker M, Aquila A L, Gullikson E M, Attwood D T, Kienberger R , Krausz F and Kleineberg U 2008 *Science* **320** 1614

[5] Strickland D and Mourou G 1985 *Opt. Commun.* **56** 219

[6] Nakajima T and Watanabe S 2006 *Opt. Lett.* **31** 1920

[7] Nakajima T and Cormier E 2007 *Opt. Lett.* **32** 2879

[8] Nakajima T 2007 *Phys. Rev.* A **75** 053409

[9] Agostini P and DiMauro L F 2004 *Rep. Prog. Phys.* **67** 813

[10] Yulin G L, Bandrauk A D and Corkum P B 2006 *Phys. Rev. Lett.* **96** 063002

[11] Keldysh L V 1964 *Zh. Eksp. Teor. Fiz* **47** 1945
Keldysh L V 1965 *Sov. Phys. JETP.* **20** 1307

[12] Faisal F H M 1973 *J. Phys.* B **6** L89

[13] Reiss H R 1980 *Phys. Rev.* A **22** 1786

[14] Reiss H R 1990 *Phys. Rev.* A **42** 1476

[15] Reiss H R 1996 *Phys. Rev.* A **54** R1765

[16] Paulus G G, Nicklich W, Xu H L, Lambropoulos P and Walther H 1994 *Phys. Rev. Lett.* **72** 2851

[17] Walker B, Sheehy B, Kulander K C and DiMauro L F 1996 *Phys. Rev. Lett.* **77** 5031

[18] Becker W, Lohr A and Kleber M 1994 *J. Phys.* B: *At. Mol. Opt. Phys.* **27** L325

[19] Becker W, Lohr A and Kleber M 1995 *Quantum Semiclass. Opt.* **7** 423

[20] Lewenstein M, Balcou P, Ivanov M Y, L'Huillier A and Corkum P B 1994 *Phys. Rev.* A **49** 2117

[21] Kumarappan V, Holmegaard L, Martiny C, Madsen C B, Kjeldsen T K, Viftrup S S, Madsen L B and Stapelfeldt H 2008 *Phys. Rev. Lett.* **100** 093006

[22] Busuladžić M, Gazibegović-Busuladžić A, Milošević D B and Becker W 2008 *Phys. Rev. Lett.* **100** 203003

[23] Bergues B, Ni Y F, Helm H and Kiyan I Y 2008 *Phys. Rev. Lett.* **95** 263002

[24] Baker S, Robinson J S, M. Lein M, Chirilă C C, Torres R, Bandulet H C, Comtois D, Kieffer J C, Villeneuve D M, Tisch J W G and Marangos J P 2008 *Phys. Rev. Lett.* **101** 053901

[25] Mairesse Y and Quéré F 2005 *Phys. Rev.* A **71** 011401(R)

[26] Kitzler M, Milosevic N, Scrinzi A, Krausz F and Brabec T 2002 *Phys. Rev. Lett.* **88** 173904

[27] Varjú K, Johnsson P, Mauritsson J, Remetter T, Ruchon T, Ni Y, Lépine F, Kling M, Khan J, Schafer K J, Vrakking M J J and L'Huillier A 2006 *J. Phys.* B **39** 3983

[28] Mishima K, Hayashi M, Yi J, Lin S H, Selzle H L and Schlag E W 2002 *Phys. Rev.* A **66** 053408

[29] Chen Z J, Morishita T, Le A T and Lin C D 2007 *Phys. Rev.* A **76** 043402

[30] Peng L Y and Starace A F 2007 *Phys. Rev.* A **76** 043401

[31] Peng L Y, Pronin E A and Starace A F 2008 *New J. Phys.* **10** 025030